



CHORUS

This is the accepted manuscript made available via CHORUS. The article has been published as:

Half-metallic magnetization plateaux

Zhihao Hao and Oleg A. Starykh

Phys. Rev. B **87**, 161109 — Published 15 April 2013

DOI: [10.1103/PhysRevB.87.161109](https://doi.org/10.1103/PhysRevB.87.161109)

Half-metallic magnetization plateaux

Zhihao Hao

Department of Physics and Astronomy, University of Waterloo, Waterloo, ON N2L 3G1, Canada

Oleg A. Starykh

Department of Physics and Astronomy, University of Utah, Salt Lake City, UT 84112, USA

(Dated: July 30, 2012)

We propose novel interaction-based routes to half-metal state for interacting electrons on two-dimensional lattices. Magnetic field applied parallel to the lattice is used to tune one of the spin densities to a particular commensurate with the lattice value in which the system spontaneously ‘locks in’ via van Hove enhanced density wave state. Electrons of opposite spin polarization retain their metallic character and provide for the half-metal state which, in addition, supports magnetization plateau in a finite interval of external magnetic field. Similar half-metal state is realized in the finite- U Hubbard model on a triangular lattice at $1/3$ of the maximum magnetization.

PACS numbers: 71.10.Fd, 72.25.-b, 75.30.-m

Spin systems supporting robust magnetization plateaux whereby macroscopic magnetization M is fixed at a rational fraction of the full (saturated) magnetization value M_{sat} in a finite interval of external magnetic field $h_1 < h < h_2$ are subject of intense experimental studies [1–5]. Typically these materials are magnetic insulators which are well described by the Heisenberg-type models with short-range exchange interactions between localized spins.

One of the best understood and studied plateau states is the up-up-down (UUD) magnetization plateau at $M = \frac{1}{3}M_{\text{sat}}$ in the triangular lattice antiferromagnet [6, 7]. It is a remarkably stable state known to survive significant spatial deformation of exchange integrals in both quantum (spin $1/2$) and classical versions of the model [8–10]. The basic reason for the stability lies in the *collinear* structure of the UUD configuration. Collinearity preserves $U(1)$ symmetry of the Hamiltonian with respect to the magnetic field axis. The only broken symmetry is then the discrete translational symmetry since the unit cell consists of two up and one down spin. This ensures the absence of the gapless (Goldstone) modes in the spectrum leading to the enhanced stability.

Since the Heisenberg model is the low-energy approximation to the large- U/t limit (t is the hopping integral and U is on-site interaction energy, see below) of the half-filled Hubbard model, the *insulating* magnetization plateau state is favored by strong electron-electron interactions. What happens to the $1/3$ magnetization plateau state as U/t is reduced and electrons delocalize is one of the key questions of our study.

A different class of magnetization plateau materials is provided by half-metallic ferromagnets [11–13] in which by virtue of peculiar electronic structure *all* conduction electrons have the same spin orientation. In their simplest version half-metallic materials are then fully saturated, $M = M_{\text{sat}}$. These materials are conductors and are well understood in terms of non-interacting electron picture [11–13].

The aim of our work is to unite these phenomena by proposing two new *interacting* routes to the *half-metallic* magnetization plateau states. Both routes require finite external (Zee-

man) magnetic field, applied parallel to the two-dimensional triangular lattice.

The *weak-coupling* route, described below first, relies on tuning density of majority (say, spin-up) electrons n_{\uparrow} to a specific value ($3/4$), commensurate with the triangular lattice, at which the Fermi surface (FS) passes van Hove points with logarithmically divergent density of states (Figure 1). Depending on the total electron density $n = n_{\uparrow} + n_{\downarrow}$, the FS of minority (spin-down) electrons may or may not be affected by the interactions, but in any case retains its metallic character. The resulting ground state is a half-metallic magnetization plateau of $M = (\frac{3}{4} - n_{\downarrow})M_{\text{sat}}$ with ferrimagnetic (up-down-down-down) collinear spin structure. M/M_{sat} is generally *irrational*. This novel state has no analogs in the large- U limit of the Hubbard model and displays coexisting *spin-* and *charge-*density wave orders. Theoretical analysis of this limit bears strong similarities with recent proposals [14–19] of collinear and chiral spin-density wave (SDW) and superconducting states of itinerant electrons on honeycomb lattice in vicinity of electron filling factors $3/8$ and $5/8$ at zero magnetization. The collinear SDW order there spontaneously breaks spin-rotational symmetry of the Hamiltonian and is accompanied by gapless collective excitations [20] which drive the competition between the collinear and chiral SDW at finite temperature [16]. This complication is absent in our problem where external magnetic field sets direction of the collinear SDW. The resulting half-metallic state breaks only discrete translational symmetry of the lattice and is stable to fluctuations of the order parameter about its mean-field value.

Next we describe the *strong coupling* (large- U) route and show that $M = \frac{1}{3}M_{\text{sat}}$ magnetization plateau ($n_{\uparrow} = 2/3, n_{\downarrow} = 1/3$), present in the $U/t \rightarrow \infty$ limit, survives down to $U_{c1}/t \approx 4.3$, which is significantly lower than the zero-magnetization critical value $U_{120^\circ}/t \approx 10$ below which the three-sublattice 120° magnetic order melts as the system transitions to a quantum spin-liquid state [21–23]. Quite interestingly, we find that in the interval $U_{c1} \leq U \leq U_{c2} \approx 4.8t$ the UUD state is a *half-metal* with mobile majority (spin-up)

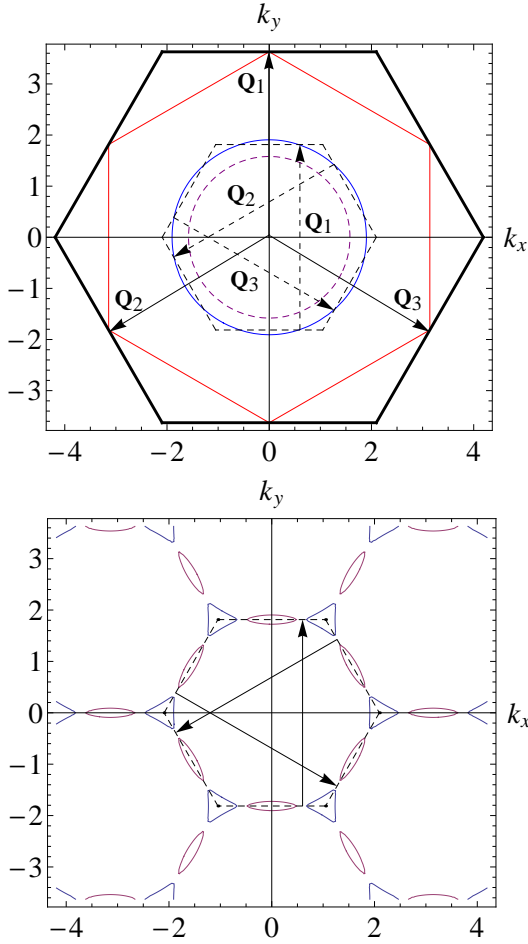


FIG. 1: (Color online) The non-interacting Fermi surfaces of spin-up and spin-down electrons (top) at 1/2 magnetization and the reconstructed Fermi surface of spin-down electrons at $y_{\perp}/t = 0.1$ (bottom). The thick black and the dashed hexagons are the first Brillouin zones under the unfolded and folded scheme. The red hexagon, the Fermi surface of the spin-up electron, is perfectly nested by linear combinations of three wave vectors (the arrows). The dashed purple circle is an example of the hot-spot-free Fermi surface of spin-down electrons in the hole doped system.

electrons.

Weak-coupling analysis is based on the extended Hubbard model on triangular lattice:

$$H = -t \sum_{\langle rr' \rangle} (c_{r\sigma}^{\dagger} c_{r'\sigma} + \text{h.c.}) + U \sum_r n_{r\uparrow} n_{r\downarrow} + V \sum_{\langle rr' \rangle} n_r n_{r'} - \sum_r \left(\mu + \frac{h\sigma}{2} \right) c_{r\sigma}^{\dagger} c_{r\sigma}. \quad (1)$$

Here $\langle rr' \rangle$ labels nearest neighbour bonds, $0 < U/t, V/t \ll 1$ are onsite and nearest neighbour repulsive interactions, respectively. For now we set the average electron density at $n = \langle n_i \rangle = \langle n_{i\uparrow} + n_{i\downarrow} \rangle = 1$.

The Zeeman field h , normalized to include the usual $g\mu_B$ factor, is tuned to produce $M = \frac{1}{2} M_{\text{sat}}$ magnetization so

that on average $n_{\uparrow} = 3/4$ and $n_{\downarrow} = 1/4$ per site. Under this condition the FS of spin-up electrons (Figure 1) is given by a perfect hexagon whose vertices, located at the M points of the first Brillouin zone (BZ), are van Hove (saddle) points of the dispersion with vanishing Fermi velocity [16]. These saddle points have the (logarithmically) diverging density of states which leads to singular susceptibility (see below). They are connected by the wave vectors $\mathbf{Q}_1 = \frac{2\pi}{\sqrt{3}} \hat{y}$ and $\mathbf{Q}_{2,3} = \mp \pi \hat{x} - \frac{\pi}{\sqrt{3}} \hat{y}$ (Fig. 1), which are halves of the corresponding reciprocal lattice vectors $\mathbf{G}_{1,2,3}$ [14]. In addition, parallel faces of the FS are perfectly nested by linear combinations of \mathbf{Q} 's. Spin-down FS is nearly circular (Fig. 1) with no special features.

The special role of the wave vectors $\mathbf{Q}_{1,2,3}$ is conveniently quantified by charge susceptibility $\chi_{\sigma}(\mathbf{q})$ of spin- σ electrons defined as

$$\chi_{\sigma}(\mathbf{q}) = \frac{1}{N} \sum_{\mathbf{k}} \frac{n_{\mathbf{k},\sigma} - n_{\mathbf{k}+\mathbf{q},\sigma}}{\epsilon_{\mathbf{k}} - \epsilon_{\mathbf{k}+\mathbf{q}}}. \quad (2)$$

Here N is the number of sites, $n_{\mathbf{k},\sigma}$ is the occupation number of fermions with spin σ and momentum \mathbf{k} and

$$\epsilon_{\mathbf{k}} = -2t \left(\cos k_x + 2 \cos \frac{k_x}{2} \cos \frac{\sqrt{3}k_y}{2} \right) \quad (3)$$

is the free-particle dispersion. Straightforward calculation, outlined in [24], shows that $\chi_{\uparrow}(\mathbf{Q}_a)$ is strongly divergent, while $\chi_{\downarrow}(\mathbf{Q}_a)$ is finite,

$$\chi_{\uparrow}(\mathbf{Q}_a) = -\frac{C_{\uparrow}}{t} \ln^2 \left(\frac{\Lambda}{q_0} \right), \quad C_{\uparrow} = \frac{1}{2\pi^2}, \quad (4)$$

$$\chi_{\downarrow}(\mathbf{Q}_a) = -\frac{C_{\downarrow}}{t}, \quad C_{\downarrow} \approx 0.136. \quad (5)$$

Here $\Lambda \sim \pi/a$ is the 'size' of the BZ (a is the lattice spacing) while $q_0 \sim 1/L$ is the microscopic cut-off which scales as the inverse linear size of the lattice $L \sim \sqrt{N}a$.

Eq. (4) suggests strong modulation of density at $\mathbf{q} = \pm \mathbf{Q}_a$ which motivates the following mean-field ansatz

$$\langle n_{r,\sigma} \rangle = \frac{2+\sigma}{4} + m_{\sigma} \sum_{a=1}^3 \cos(\mathbf{Q}_a \cdot \mathbf{r}), \quad (6)$$

where index σ describes two spin projections, $\sigma = \uparrow = +1$ and $\sigma = \downarrow = -1$. The average electron densities $n_{\sigma} = \sum_r \langle n_{r,\sigma} \rangle / N$ are not affected by finite order parameters m_{σ} , and $n_{\uparrow} = 3/4$, while $n_{\downarrow} = 1/4$. Ansatz (6) allows us to approximate (1) as

$$H = \sum_{\mathbf{k},\sigma} (\epsilon_{\mathbf{k}} - \mu_{\sigma}) c_{\mathbf{k}\sigma}^{\dagger} c_{\mathbf{k}\sigma} + \frac{1}{2} \sum_{\mathbf{k},\sigma,a} y_{\sigma} (c_{\mathbf{k}\sigma}^{\dagger} c_{\mathbf{k}+\mathbf{Q}_a\sigma} + \text{h.c.}) + 3NV(m_{\uparrow} + m_{\downarrow})^2 - 3NUm_{\uparrow}m_{\downarrow}, \quad (7)$$

$$y_{\sigma} = Um_{-\sigma} - 2V(m_{\uparrow} + m_{\downarrow}), \quad (8)$$

The amplitudes of density modulation of spin- σ electrons are

determined self-consistently

$$\begin{aligned} m_\sigma &= \frac{1}{3N} \sum_{\mathbf{r}, a} \cos(\mathbf{Q}_a \cdot \mathbf{r}) \langle n_{\mathbf{r}, \sigma} \rangle \\ &= \frac{y_\sigma}{3N} \sum_{\mathbf{k}, a} \frac{n_{\mathbf{k}, \sigma} - n_{\mathbf{k} + \mathbf{Q}_a, \sigma}}{\tilde{\epsilon}_{\mathbf{k}} - \tilde{\epsilon}_{\mathbf{k} + \mathbf{Q}_a}} = y_\sigma \chi_\sigma(\mathbf{Q}_a), \end{aligned} \quad (9)$$

where dispersion $\tilde{\epsilon}_{\mathbf{k}}$ is determined by the mean-field Hamiltonian (7). We find $m_\downarrow = C_\downarrow(V - U/2)m_\uparrow/t$, which means $|m_\downarrow| \ll |m_\uparrow|$, and

$$\frac{C_\uparrow}{t} \ln^2\left(\frac{\Lambda}{q_\uparrow}\right) = \left(V + \frac{C_\downarrow}{t}(V - \frac{U}{2})^2\right)^{-1}. \quad (10)$$

The main effect of interaction y_\uparrow in (7) is to provide an infrared cut-off $q_\uparrow \sim |y_\uparrow/t|^{1/2}$ in the susceptibility (4) of spin-up electrons at the van Hove points. This leads to the final result

$$\begin{aligned} m_\uparrow &= -\frac{\Lambda^2 t}{V + \frac{C_\downarrow}{t}(V - U/2)^2} \\ &\times \exp\left(-\sqrt{\frac{4t}{C_\uparrow[V + \frac{C_\downarrow}{t}(V - U/2)^2]}}\right). \end{aligned} \quad (11)$$

Non-analytic dependence of m on interaction amplitudes U, V is determined by van Hove points. The sign of m_\uparrow is chosen such that the FS of spin-up electrons is gapped for *all* momenta. We checked that the opposite sign leads to a quadratic touching of the top two bands at Γ point and results in a state of higher energy [24].

Equations (6) and (11) show that the ground state is a superposition of commensurate charge-density and collinear spin-density waves. $\sum_{a=1}^3 \cos(\mathbf{Q}_a \cdot \mathbf{r})$ takes values 3, -1, -1, -1 on the sites of triangular lattice $\mathbf{r} = (x, y) = d_1 \mathbf{a}_1 + d_2 \mathbf{a}_2$, where $\mathbf{a}_1 = (1, 0)$ and $\mathbf{a}_2 = (1/2, \sqrt{3}/2)$ are elementary lattice vectors and $d_{1,2}$ are integers. We stress that the perfectly nested FS of spin-up electrons is crucial for the spin-up electrons to be gapped at arbitrary weak interaction.

In the absence of direct density-density interaction, $V = 0$, the order parameter scales as $m \sim \exp(-\text{const}/U)$. The density wave of spin-up electrons in this case is driven by the effective interaction $\propto \chi_\downarrow U^2$ mediated by spin-down electrons, since the onsite repulsion U only couples electrons of opposite spins. A small finite $V \geq U^2/t$, see (11), changes this scaling to a much stronger dependence $m \sim \exp(-\text{const}/\sqrt{V})$.

The band structure of spin-down electrons is also modified as (7) shows. For finite y_\downarrow , while the spin-down electrons remain gapless, the ‘hot spots’ on the spin-down FS (which are the points connected by \mathbf{Q}_a) are gapped and the FS is reconstructed (Figure 1). By reducing the density of spin-down electrons n_\downarrow below 1/4, while maintaining that of spin-up ones at the perfect nesting condition $n_\uparrow = 3/4$, one reduce the spin-down FS below the critical volume to fit inside the reduced Brillouin zone (dashed hexagon in Fig. 1), which is 4 times smaller than the original one, and the hot spots disappear altogether. This happens for $n_{\text{cr}} < 0.976$ (Figure 1), *i.e.*

$n_{\text{cr}\downarrow} < 0.226$. Under this condition, and for weak interactions $U, V \ll t$, the FS of spin-down electrons is not affected at all. In either case, the result is a *half-metal* where spin fluctuations are gapped and *all* conducting electrons have spin opposite to the direction of the external field.

Relaxing half-filling $n = 1$ condition makes the proposed half-metal state easier to achieve experimentally. The idea is to first adjust the total electron density to be sufficiently close, but not quite at, van Hove singularity. Next, apply magnetic field to drive (say, spin \uparrow) towards density-wave instability while at the same time de-tuning spin- \downarrow subsystem away from it. As shown in [24] for the two lattice geometries, square and honeycomb (graphene), choosing total density properly one can achieve the desired half-metal state with relatively small field $h \leq 0.02t$. Taking $t = 0.3$ eV results in the estimate $h \sim 100$ T.

Strong coupling limit. We turn to the question of $M = \frac{1}{3}M_{\text{sat}}$ plateau which exists in the opposite limit of strong interactions, $U \gg t$. To make connection with the insulating magnetization plateau phase of the Heisenberg spin model we set $V = 0$, keeping total density $n = 1$ and introduce the following mean-field ansatz:

$$\langle n_{\mathbf{r}\sigma} \rangle = \frac{1}{2} + \frac{\sigma}{6} - 2\eta_\sigma \cos(\mathbf{Q} \cdot \mathbf{r}) \quad (12)$$

where $\mathbf{Q} = \frac{4\pi}{3}\hat{x}$ describes the UUD pattern. ($\cos(\mathbf{Q} \cdot \mathbf{r})$ takes values 1, $-1/2$, $-1/2$ on the triangular lattice.) Parameters η_σ are determined self-consistently by the equations similar to (9). Solving them numerically we find discontinuous jump of η_σ from zero to finite values when $U \geq 4.30t$ for a range of h . η_\uparrow and η_\downarrow are in general different so that the system displays a co-existence of the spin-density and charge-density wave orders [24]. Interestingly, it is the spin-down electrons that are gapped while the spin-up electrons remain gapless around the Fermi energy (Figure 2). Spin-down electrons fill completely the lowest of the three bands $\omega_\downarrow(\mathbf{k})$ in the folded Brillouin zone, while the spin-up ones fill the two lowest bands $\omega_\uparrow(\mathbf{k})$. For even stronger interaction $U > 4.80t$, the two upper spin-up bands also get separated by a gap which turns the half-metal state into an insulator with collinear UUD pattern of local magnetization.

We compared the energy of the half-metal state with the uniformly magnetized transverse spin-density wave state, *i.e.* ‘‘cone’’ state in magnetic language. This state is characterized by the longitudinal $\langle S_{\mathbf{r}}^z \rangle = M$ and transverse $\langle S_{\mathbf{q}}^+ \rangle = m_0 e^{i\mathbf{q} \cdot \mathbf{r}}$ magnetizations [25, 26], where the ordering wave vector \mathbf{q} is generally incommensurate. We determined that the half-metal state has a lower energy for $4.45t \leq U \leq 4.80t$ [24]. The mean-field phase diagram is shown in Figure 3. Both half-metal and UUD insulator phases are plateau states with $M = \frac{1}{3}M_{\text{sat}}$.

Discussion: we described two general ways to induce half-metal states through a combination of electronic interactions and a finite Zeeman field. Our work provides new avenues to half-metallic states which have potential applications in future spin-dependent electronics. Despite our focus on the

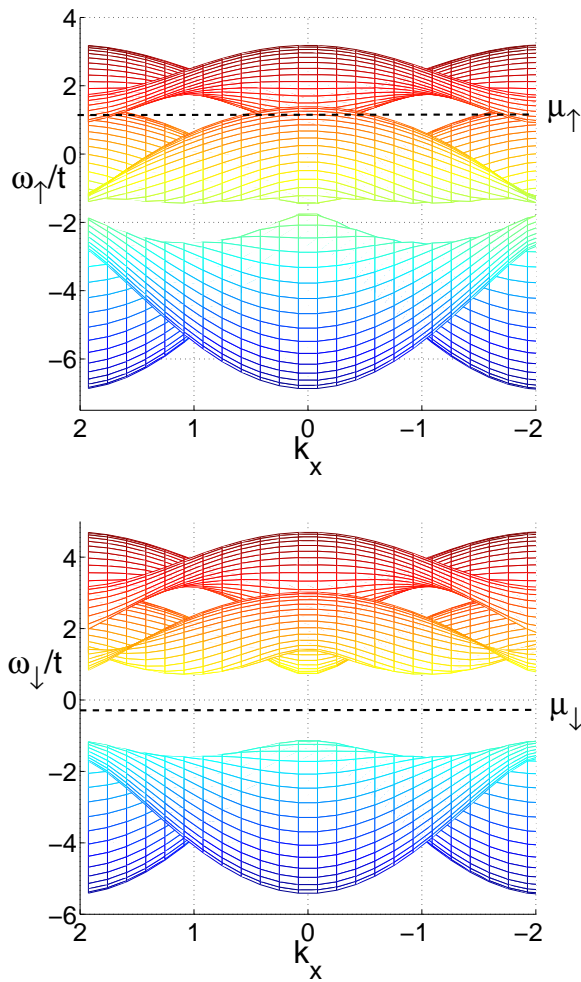


FIG. 2: (Color online) The spin-up (top) and spin-down (bottom) bands of the half-metal state at $1/3$ magnetization at $U = 4.60t$. The graph shows projections of two-dimensional bands onto k_x axis for 30 discrete k_y . The Fermi energies $\mu_\sigma = \mu + \sigma(h/2 + U/6)$ are black-dash lines.

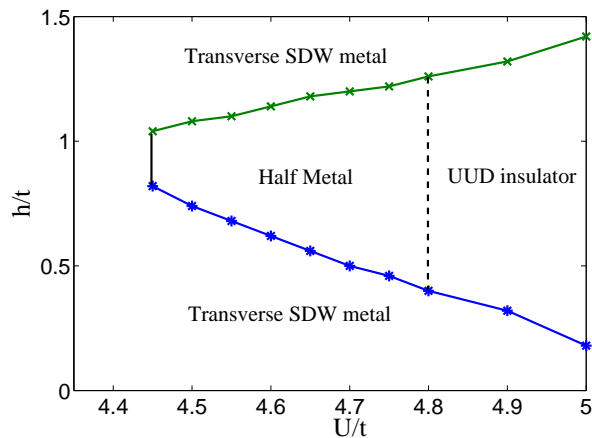


FIG. 3: (Color online) The mean-field phase boundaries of the half-metal and insulating states at $M = 1/3 M_{\text{sat}}$ on triangular lattice. Solid (dashed) lines denote first (second) order transitions.

Hubbard-Heisenberg model on the triangular lattice, both of the proposed mechanisms can be generalized to other lattice geometries. We suggest that doped graphene, which is actively investigated for van Hove - related instabilities [27, 28], provides convenient setting for searching for the field-induced half-metallic plateau state.

Our proposal can also be realized in Kondo lattice systems where the Zeeman field is provided by exchange couplings between the itinerant electrons and ferrimagnetically ordered local moments, see e.g. [14, 29], as well as in cold atom systems [30, 31] where it may be easier to achieve the required spin population imbalance.

Magnetic field control of the half-metallic phase may be useful for creating switchable interfaces between half-metal and noncentrosymmetric superconductor which have been argued to support Majorana bound states [32].

It is worth noting close physical similarity between our proposal and the previously proposed one-dimensional ‘Coulomb drag’ setup [33] where role of the lattice is played by the electrons in an active wire interactions with which gap out one of the spin projections in the passive wire.

Several interesting theoretical questions can be asked regarding the half-metal state. First of all, the metal-insulator transition between a half-metal and a Mott insulator, found here at $U/t \approx 4.8$, represents Mott transition not affected by (gapped) spin fluctuations. Understanding it in details may lead to a better characterization of the general Mott transition. Half metal states are adjacent to many other interesting quantum phases including recently proposed $d + id$ chiral superconducting state [15]. If we dope such state with holes while keeping the FS of spin-up electrons perfectly nested by a Zeeman field, we will eventually obtain a half-metal. Understanding how quantum phase transition(s) between these different phases happen is an interesting question left for future studies.

We thank A. V. Chubukov, L. I. Glazman, M. J. P. Gingras, E. G. Mishchenko, M. E. Raikh and O. V. Tchernyshyov for useful discussions. This work was initiated at the Max-Planck Institute for the Physics of Complex Systems during the Advanced Study Group on ‘‘Unconventional Magnetism in High Field’’, which we thank for hospitality. The work is supported by NSF through Grant No. DMR-1206774 (O.A.S.) and by NSERC of Canada (Z.H.).

-
- [1] K. Kodama, M. Takigawa, M. Horvatic, C. Berthier, H. Kageyama, Y. Ueda, S. Miyahara, F. Becca, and F. Mila, *Science* **298**, 395 (2002).
- [2] H. Kikuchi, Y. Fujii, M. Chiba, S. Mitsudo, T. Idehara, T. Tonegawa, K. Okamoto, T. Sakai, T. Kuwai, and H. Ohta, *Phys. Rev. Lett.* **94**, 227201 (2005).
- [3] H. Ueda, H. A. Katori, H. Mitamura, T. Goto, and H. Takagi, *Phys. Rev. Lett.* **94**, 047202 (2005).
- [4] N. A. Fortune, S. T. Hannahs, Y. Yoshida, T. E. Sherline, T. Ono, H. Tanaka, and Y. Takano, *Phys. Rev. Lett.* **102**, 257201 (2009).
- [5] H. Nema, A. Yamaguchi, T. Hayakawa, and H. Ishimoto, *Phys. Rev. Lett.* **102**, 075301 (2009).
- [6] H. Kawamura and S. Miyashita, *Journal of the Physical Society of Japan* **54**, 4530 (1985).
- [7] A. V. Chubukov and D. I. Golosov, *Journal of Physics: Condensed Matter* **3**, 69 (1991).
- [8] J. Alicea, A. V. Chubukov, and O. A. Starykh, *Phys. Rev. Lett.* **102**, 137201 (2009).
- [9] C. Griset, S. Head, J. Alicea, and O. A. Starykh, *Phys. Rev. B* **84**, 245108 (2011).
- [10] R. Chen, H. Ju, H.-C. Jiang, O. A. Starykh, and L. Balents, *ArXiv e-prints* (2012), 1211.1676.
- [11] R. A. de Groot, F. M. Mueller, P. G. v. Engen, and K. H. J. Buschow, *Phys. Rev. Lett.* **50**, 2024 (1983).
- [12] K. Schwarz, *Journal of Physics F: Metal Physics* **16**, L211 (1986).
- [13] M. I. Katsnelson, V. Y. Irkhin, L. Chioncel, A. I. Lichtenstein, and R. A. de Groot, *Rev. Mod. Phys.* **80**, 315 (2008).
- [14] I. Martin and C. D. Batista, *Phys. Rev. Lett.* **101**, 156402 (2008).
- [15] R. Nandkishore, L. S. Levitov, and A. V. Chubukov, *Nat Phys* **8**, 158 (2012).
- [16] R. Nandkishore, G.-W. Chern, and A. V. Chubukov, *Phys. Rev. Lett.* **108**, 227204 (2012).
- [17] G.-W. Chern, R. M. Fernandes, R. Nandkishore, and A. V. Chubukov, *ArXiv e-prints* (2012), 1203.5776.
- [18] G.-W. Chern and C. D. Batista, *ArXiv e-prints* (2012), 1204.5737.
- [19] M. L. Kiesel, C. Platt, W. Hanke, D. A. Abanin, and R. Thomale, *Phys. Rev. B* **86**, 020507 (2012).
- [20] M. A. Metlitski and S. Sachdev, *Phys. Rev. B* **82**, 075128 (2010).
- [21] H. Morita, S. Watanabe, and M. Imada, *Journal of the Physical Society of Japan* **71**, 2109 (2002).
- [22] P. Sahebsara and D. Sénéchal, *Phys. Rev. Lett.* **100**, 136402 (2008).
- [23] H.-Y. Yang, A. M. Läuchli, F. Mila, and K. P. Schmidt, *Phys. Rev. Lett.* **105**, 267204 (2010).
- [24] See Supplementary Material for more details.
- [25] H. R. Krishnamurthy, C. Jayaprakash, S. Sarker, and W. Wenzel, *Phys. Rev. Lett.* **64**, 950 (1990).
- [26] C. Jayaprakash, H. R. Krishnamurthy, S. Sarker, and W. Wenzel, *Europhysics Letters* **15**, 625 (1991).
- [27] J. L. McChesney, A. Bostwick, T. Ohta, T. Seyller, K. Horn, J. González, and E. Rotenberg, *Phys. Rev. Lett.* **104**, 136803 (2010).
- [28] D. K. Efetov and P. Kim, *Phys. Rev. Lett.* **105**, 256805 (2010).
- [29] M. Kreissl and W. Nolting, *Phys. Rev. B* **72**, 245117 (2005).
- [30] G. B. Partridge, W. Li, R. I. Kamar, Y.-A. Liao, and R. G. Hulet, *Science* **311**, 503 (2006).
- [31] M. W. Zwierlein, A. Schirotzek, C. H. Schunck, and W. Ketterle, *Science* **311**, 492 (2006).
- [32] M. Duckheim and P. W. Brouwer, *Phys. Rev. B* **83**, 054513 (2011).
- [33] M. Pustilnik, E. G. Mishchenko, and O. A. Starykh, *Phys. Rev. Lett.* **97**, 246803 (2006).